

A Spatial Repetitive Controller Applied to an Aeroelastic Model for Wind Turbines

Riccardo Fratini, Riccardo Santini, Jacopo Serafini, Massimo Gennaretti, Stefano Panzieri

Abstract—This paper presents a nonlinear differential model, for a three-bladed horizontal axis wind turbine (HAWT) suited for control applications. It is based on a 8-dofs, lumped parameters structural dynamics coupled with a quasi-steady sectional aerodynamics. In particular, using the Euler-Lagrange Equation (Energetic Variation approach), the authors derive, and successively validate, such model. For the derivation of the aerodynamic model, the Greenbergs theory, an extension of the theory proposed by Theodorsen to the case of thin airfoils undergoing pulsating flows, is used. Specifically, in this work, the authors restricted that theory under the hypothesis of low perturbation reduced frequency k , which causes the lift deficiency function $C(k)$ to be real and equal to 1. Furthermore, the expressions of the aerodynamic loads are obtained using the quasi-steady strip theory (Hodges and Ormiston), as a function of the chordwise and normal components of relative velocity between flow and airfoil U_t , U_p , their derivatives, and section angular velocity $\dot{\epsilon}$. For the validation of the proposed model, the authors carried out open and closed-loop simulations of a 5 MW HAWT, characterized by radius $R = 61.5$ m and by mean chord $c = 3$ m, with a nominal angular velocity $\Omega_n = 1.266 \text{ rad/sec}$. The first analysis performed is the steady state solution, where a uniform wind $V_w = 11.4$ m/s is considered and a collective pitch angle $\theta = 0.88^\circ$ is imposed. During this step, the authors noticed that the proposed model is intrinsically periodic due to the effect of the wind and of the gravitational force. In order to reject this periodic trend in the model dynamics, the authors propose a collective repetitive control algorithm coupled with a PD controller. In particular, when the reference command to be tracked and/or the disturbance to be rejected are periodic signals with a fixed period, the repetitive control strategies can be applied due to their high precision, simple implementation and little performance dependency on system parameters. The functional scheme of a repetitive controller is quite simple and, given a periodic reference command, is composed of a control block $C_{rc}(s)$ usually added to an existing feedback control system. The control block contains a free time-delay system $e^{\tau s}$ in a positive feedback loop, and a low-pass filter $q(s)$. It should be noticed that, while the time delay term reduces the stability margin, on the other hand the low pass filter is added to ensure stability. It is worth noting that, in this work, the authors propose a phase shifting for the controller and the delay system has been modified as $e^{-(T-\gamma_k)}$, where T is the period of the signal and γ_k is a phase shifting of k samples of the same periodic signal. It should be noticed that, the phase shifting technique is particularly useful in non-minimum phase systems, such as flexible structures. In fact, using the phase shifting, the iterative algorithm could reach the convergence also at high frequencies. Notice that, in our case study, the shifting of k samples depends both on the rotor angular velocity Ω and on the rotor azimuth angle Ψ : we refer to this controller as a *spatial repetitive controller*. The collective repetitive controller has also been coupled with a

$C(s) = PD(s)$, in order to dampen oscillations of the blades. The performance of the *spatial repetitive controller* is compared with an industrial PI controller. In particular, starting from wind speed velocity $V_w = 11.4$ m/s the controller is asked to maintain the nominal angular velocity $\Omega_n = 1.266 \text{ rad/s}$ after an instantaneous increase of wind speed ($V_w = 15$ m/s). Then, a purely periodic external disturbance is introduced in order to stress the capabilities of the repetitive controller. The results of the simulations show that, contrary to a simple PI controller, the spatial repetitive-PD controller has the capability to reject both external disturbances and periodic trend in the model dynamics. Finally, the nominal value of the angular velocity is reached, in accordance with results obtained with commercial software for a turbine of the same type.

Keywords—Wind turbines, aeroelasticity, repetitive control, periodic systems.

I. INTRODUCTION

HAWT control is crucial for both increasing performance (power harvested from wind and its quality) and avoiding excessive stresses on components. Indeed, both wind and torque are time-varying, due to periodic and non-periodic effects. In particular, wind over turbine blades is strongly affected by terrain boundary layer, which causes periodicity in aerodynamic boundary conditions and then on loads acting on rotor blades. If the blades are not controlled, this periodicity induces high vibratory level, as well as reduction of power generated. The most effective and multipurpose way to control an HAWT is changing blade pitch in order to correct the aerodynamic incidence, while other control strategies (as yaw or torque control) are mainly aimed to avoid excessive rotational speed. Conversely, acting on blade pitch allows to reduce vibratory loads and to regulate generated torque at the same time.

Related Work

While many models for HAWT simulation and control are oversimplified and condensed (few dofs, coefficient-based aerodynamics, no direct simulation, rigid body assumption) [1], detailed analysis and design of wind turbines relies on adequate aerodynamics and structural dynamics rotor modeling, including application of suitable techniques for space and time aeroelastic system integration. The development of suitable models for wind turbines, usually involves well assessed engineering methods based on enhanced Blade Element Momentum Theory (BEMT) techniques, that include tuned-up corrections to model blade tip flow, wake dynamic inflow and dynamic stall [2]. More recently, Computational Fluid Dynamic (CFD) tools based on RANSE (Reynolds-Averaged Navier-Stokes

This work was not supported by any organization

M. Gennaretti, S. Panzieri and J. Serafini are with Faculty of Mechanical and Industrial Engineering, Roma Tre University, 00146, Roma, Italy.

R. Santini is with Faculty of Mechanical and Industrial Engineering, Roma Tre University, 00146, Roma, Italy (e-mail: riccardo.fratini@uniroma3.it).

Equations), DES (Detached Eddy Simulation) and LES (Large Eddy Simulation) aerodynamics solvers have shown the capability to achieve a physically consistent description of turbine flow-field, thus interest in coupled CFD-CSD techniques is increasing as well [3], [4]. Nevertheless, due to the high computational costs, they are not well suited for aeroelastic analyses in practical preliminary design and aero-servo-elastic applications. In this scenario, three-dimensional incompressible, potential, attached flows [5]-[7] solvers represent an advanced convenient alternative to BEMT codes. Other works, instead, only focused on a simple reduced non-linear model using finite-element multibody procedures [8], [9]. A drawback of these methods is that, even if they take into account the complete non-linear model of the turbine, only numerical solutions may be achieved.

On the control side, most solutions adopted nowadays by the manufacturers revolve around collective or cyclic pitch using classic control techniques. In the recent literature on wind turbine control, different types of controller have been studied. In [10] a torque controller that incorporates approximate-angular-acceleration feedback is proposed, to improve efficiency in presence of unsteady wind. Individual pitch control and field tests to assess the viability of such philosophy are studied, for instance, in [11], [12]. In [13] a multiple model robust control strategy is considered, and a fault tolerant pitch control is proposed to reject faults in a turbine pitch actuator. Moreover, model predictive control (MPC) techniques are active research topics in this field and recent studies have been shown promising results [9], [14], [15]. Finally, repetitive control strategies for wind turbine have been proposed in [15]-[17] when the reference command to be tracked and/or the disturbance to be rejected are periodic signals with a fixed period.

Paper Contributions

The contribution of this paper is twofold. First, the authors propose and validate a mid-fidelity nonlinear model composed of eight differential equations in eight variables for a three-blade HAWT wind turbine. Second, they propose a *spatial* collective repetitive control algorithm coupled with a PD controller in order to reject periodic trends in the model dynamics.

II. WIND TURBINE MODEL

In deriving the aeroelastic model of an horizontal-axis wind turbine, the authors moved from Euler-Lagrange differential equation (*Energetic Variational Approach*)

$$\frac{d}{dt} \left(\frac{\partial \mathcal{T}}{\partial \dot{q}_i} \right) - \frac{\partial (\mathcal{T} - \mathcal{U})}{\partial q_i} = F_i \quad \forall i = 1, \dots, n. \quad (1)$$

where $\mathcal{T} = \mathcal{T}(\dot{\mathbf{q}}, \mathbf{q})$ and $\mathcal{U} = \mathcal{U}(\mathbf{q})$ are the kinetic and potential energy, respectively, $F_i = F_i(\ddot{\mathbf{q}}, \dot{\mathbf{q}}, \mathbf{q})$ are the generalized forces and \mathbf{q} is the vector collecting the generalized coordinates q_i , which include rigid and elastic dofs. Here, eight degrees of freedom providing a semi-rigid (lumped parameters) model for the aero-elasticity of rotor-pylon system of a three-bladed HAWT are considered.

In particular,

$$q_i = \begin{cases} q_1 & = z_p; \\ q_{2,3,4} & = \beta_{1,2,3}; \\ q_{5,6,7} & = \theta_{1,2,3}; \\ q_8 & = \Psi. \end{cases} \quad (2)$$

where z_p represents the tower fore-aft elastic motion, β and θ are, respectively, flap and pitch angle of each blade, and Ψ is the azimuthal position of reference blade. The total kinetic energy \mathcal{T} may be expressed as

$$\begin{aligned} \mathcal{T} = & \frac{1}{2} \bar{v}_{g_n}^T(\dot{\mathbf{q}}, \mathbf{q}) m_{tot} \bar{v}_{g_n}(\dot{\mathbf{q}}, \mathbf{q}) + \\ & + \frac{1}{2} \sum_{i=1}^3 \bar{v}_{g_{b_i}}^T(\dot{\mathbf{q}}, \mathbf{q}) m_b \bar{v}_{g_{b_i}}(\dot{\mathbf{q}}, \mathbf{q}) + \\ & + \frac{1}{2} \sum_{i=1}^3 \bar{\omega}_{b_i}^T(\dot{\mathbf{q}}, \mathbf{q}) J_{g_b} \bar{\omega}_{b_i}(\dot{\mathbf{q}}, \mathbf{q}) \end{aligned} \quad (3)$$

where \bar{v}_{g_n} represents the velocity of the nacelle center of gravity, m_{tot} is the sum of the nacelle and pylon mass, $\bar{v}_{g_{b_i}}$ and $\bar{\omega}_{b_i}$ are the i -th blade linear and flapping angular velocities, whereas m_b and J_{g_b} represent, respectively, blade mass and matrix of inertia with respect to center of gravity. Note that \bar{v}_{g_n} , $\bar{v}_{g_{b_i}}$ and $\bar{\omega}_{b_i}$ may be easily expressed as function of $\mathbf{q}, \dot{\mathbf{q}}$ exploiting rigid body motion relations. The total potential energy \mathcal{U} is the sum of gravitational and elastic contributions (\mathcal{U}_g and \mathcal{U}_e , respectively), *i.e.*

$$\mathcal{U} = \mathcal{U}_g + \mathcal{U}_e, \quad (4)$$

In particular, the elastic energy is associated to the springs acting on z_p , β_i and θ_i dofs. These terms read as

$$\begin{aligned} \mathcal{U}_g &= \sum_{i=1}^3 U_{b_i} = \sum_{i=1}^3 -m_b g \sin \Psi x_{g_b} \cos \beta_i, \\ \mathcal{U}_e &= \frac{1}{2} k_p z_p^2 + \frac{1}{2} \sum_{i=1}^3 k_{\beta_i} \beta_i^2 + \frac{1}{2} \sum_{i=1}^3 k_{\theta_i} \theta_i^2, \end{aligned} \quad (5)$$

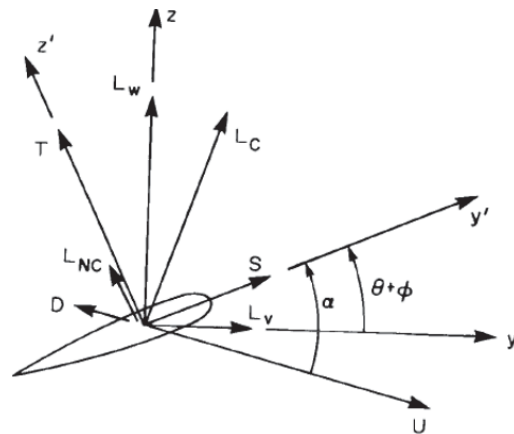


Fig. 1 Section velocity, from [20]

where m_b is the mass of the rotor blade and x_{g_b} is the radial position of the blade center of mass with respect to the flapping hinge. Now, under the assumption of small

pitching and flapping angles, *i.e.* $\sin(\beta_i, \theta_i) \approx \beta_i, \theta_i$ and $\cos(\beta_i, \theta_i) \approx 1$, and substituting (3) and (5) in (1) one obtains the following nonlinear system

$$\begin{aligned}
 m_{tot} \ddot{z}_p - \sum_{i=1}^3 m_b x_{g_b} \ddot{\beta}_i^2 + k_p z_p &= \sum_{i=1}^3 \int_0^L L_{w_i} dr \\
 J_{o_y} \ddot{\beta}_1 - m_b x_{g_b} \ddot{z}_p + (J_{o_y} \Omega^2 + m_b x_{g_b} f \Omega^2 + k_{\beta_1}) \beta_1 + \\
 -m_b x_{g_b} g \sin \Psi_1 - J_{g_x} \dot{\Omega} \theta_1 &= \int_0^L L_{w_1} r dr \\
 J_{o_y} \ddot{\beta}_2 - m_b x_{g_b} \ddot{z}_p + (J_{o_y} \Omega^2 + m_b x_{g_b} f \Omega^2 + k_{\beta_2}) \beta_2 + \\
 -m_b x_{g_b} g \sin \Psi_2 - J_{g_x} \dot{\Omega} \theta_2 &= \int_0^L L_{w_2} r dr \\
 J_{o_y} \ddot{\beta}_3 - m_b x_{g_b} \ddot{z}_p + (J_{o_y} \Omega^2 + m_b x_{g_b} f \Omega^2 + k_{\beta_3}) \beta_3 + \\
 -m_b x_{g_b} g \sin \Psi_3 - J_{g_x} \dot{\Omega} \theta_3 &= \int_0^L L_{w_3} r dr \quad (6) \\
 \sum_{i=1}^3 [m_b f^2 + J_{o_z} + 2m_b x_{g_b} f] \dot{\Omega} + \\
 -2 \sum_{i=1}^3 J_{o_y} \Omega \dot{\beta}_i \beta_i &= \sum_{i=1}^3 \int_0^L L_{v_i} (r + f) dr \\
 J_{g_x} \dot{\theta}_1 + J_{g_x} \Omega^2 \theta_1 - J_{g_x} \beta_1 \dot{\Omega} &= \int_0^L M_{\phi_2} dr + C_{c_1} \\
 J_{g_x} \dot{\theta}_2 + J_{g_x} \Omega^2 \theta_2 - J_{g_x} \beta_2 \dot{\Omega} &= \int_0^L M_{\phi_2} dr + C_{c_2} \\
 J_{g_x} \dot{\theta}_3 + J_{g_x} \Omega^2 \theta_3 - J_{g_x} \beta_3 \dot{\Omega} &= \int_0^L M_{\phi_3} dr + C_{c_3}
 \end{aligned}$$

where $\Omega = \dot{\Psi}$ is the rotor angular velocity, f is the distance between flapping hinge and rotation axis, and g is the gravitational acceleration. Although small, the effect of gravity is one of the sources of system periodicity.

The aerodynamic model chosen for this study is derived from the Greenberg's theory [18], an extension of Theodorsen's theory [19] to the case of thin airfoils undergoing pulsating flows. Here, the authors restricted that theory under the hypothesis of low perturbation reduced frequency k , which causes the *lift deficiency function* $C(k)$ [19] to be real and equal to 1 (*i.e.*, no delay between boundary conditions and resulting load is present). The sectional aerodynamic lift force and moment are then sum of two contributions: the former is the circulatory component due to the circulation around the airfoil and the latter is the non-circulatory part, also present on non-lifting bodies. It is worth noting that, while circulatory lift and moment exist also in unsteadiness, non-circulatory contribution is only due to unsteadiness. Furthermore, a simple expression for skin friction and form drag is added through the inclusion of drag coefficient, C_{d0} . Following the approach proposed by Hodges and Ormiston [20], the authors expressed aerodynamic loads as a function of the chordwise and normal components of relative velocity between flow and airfoil U_t, U_p , their derivatives, and section angular velocity $\dot{\epsilon}$.

Expressing these velocities in terms of system dofs (exploiting rigid body motion relations) results in the following expression for aerodynamic in-plane (L_v) and out-of-plane (L_w) sectional forces and moment (M_ϕ)

generated by each blade (see Fig. 1), appearing in (6)

$$\begin{aligned}
 L_v &\approx \frac{2\pi\rho c}{2} [V_w(V_w - \Omega r \theta)(S^2 \phi C \phi + C^3 \phi) + \\
 &\quad - \frac{C_{d0} \Omega^2 r^2 C^3 \phi}{2\pi} - \Omega r(r \dot{\beta} + V_w - \dot{z}_p) \\
 &\quad (S \phi C^2 \phi + S^3 \phi) - \frac{c}{4} \dot{\Omega} r S^2 \phi] \\
 L_w &\approx \frac{2\pi\rho c}{2} [\Omega^2 r(r + 2f)(S \phi C^2 \phi + S^3 \phi) + \\
 &\quad - \frac{C_{d0} \Omega^2 r^2 S \phi C^2 \phi}{2\pi} + \Omega r(\dot{z}_p + \Omega r \theta - V_w + \\
 &\quad - r \dot{\beta})(S^2 \phi C \phi + C^3 \phi) + \\
 &\quad \frac{c}{4} \dot{\Omega} r S \phi C \phi + 2\Omega r f S \phi C^2 \phi] \\
 M_\phi &\approx - \frac{2\pi\rho c}{2} \left(\frac{c}{4}\right)^2 [\dot{\Omega}(r + f) S \phi + (\Omega^2 r \beta + \dot{z}_p + \\
 &\quad \dot{\Omega} r \theta + 2\Omega r \dot{\theta} - \ddot{\beta} r - V_w C \phi)] \quad (7)
 \end{aligned}$$

where c is blade chord, ρ is air density, V_w is the wind velocity, ϕ is blade structural twist, whereas S and C are abbreviation for $\sin()$ and $\cos()$. It is worth noting that, if a non-uniform inflow is considered (*e.g.*, due to terrain boundary layer) this results in strong periodicity of the system.

III. CONTROL OBJECTIVES AND STRATEGIES

In this section the control objective and strategies for the wind turbines are outlined. In particular, the repetitive control strategy is introduced and the proposed *spatial* repetitive controller algorithm is described.

A. Control Objective

A wind turbine is essentially a device that captures part of the wind energy and converts it into useful work. To achieve this goal, several factors can be taken into account:

- **Energy capture:** Energy maximization with safe operation restrictions (*e.g.*, rated power, rated speed and cut-off wind speed);
- **Mechanical loads:** Protect the wind turbine against excessive dynamic mechanical loads;
- **Power quality:** Provide good Power Quality to comply with the standards of grid connected wind turbines.

In addition, different working condition are possible for a wind turbine, such as fixed-speed/variable-speed or fixed-pitch/variable-pitch. These strategies are usually combined together, in order to achieve the control objectives over the full range of operational wind speeds.

B. Control Strategies

Wind turbines usually have at least three different possible control actuators: blade pitch, generator torque, and machine yaw [1], [21]-[23]. The blade pitch controller is the most effective one in the control of the aerodynamic loads. We

can find two configurations for this type of controller: the collective and the independent pitch control. In the first configuration the angle of each blade is adjusted identically, whereas for the independent pitch control the angle is adjusted independently of the other blades. The generator torque, instead, is most often used in region 2 to maintain turbine operation at maximum power coefficient C_p . It can also be used to add damping to the drive-train torsion modes of the turbine in region 3. In addition, the power output of the turbine can be limited by yawing the machine out of the wind, thereby decreasing the projected rotor area and reducing power. Most often, yaw control is used only to respond to changes in wind direction in an attempt to reduce the yaw error (the angle between the mean wind direction and the direction of orientation of the turbine) and thereby maximize power. In this paper, the authors choose to work with a fixed-speed/variable-speed mode such that the wind turbine can reach the maximum power conversion only at a specific wind speed. In particular, the power has been limited, above the rated wind speed, using the well known pitch-to-feather approach. With this method, it is possible to stop the rotor when the wind exceeds the maximum rated speed. Specifically, the controller acts increasing the pitch angle while the trim angle decreases.

C. Repetitive Control

Tracking reference commands without a steady state error and reject disturbances acting on the control variables, are well known basic requirements in controls systems. In addition, in many practical applications (such as high accuracy trajectory control in servomechanisms, robot control, altitude stabilization of satellites, current compensation in active filters and control of rotation mechanisms), the control tasks are often of a repetitive nature. Due to the increasingly high demand on the productivity and quality, one of the most challenging tasks in the last years, has become the high precision control of such kind of systems. Hence, instead the classical tuning of general servo controllers such as PID or state feedback controllers, a special class of techniques may be considered to handle with these periodic signals. In particular, when the reference command to be tracked and/or the disturbance to be rejected are periodic signals with a fixed period, the *repetitive control* strategy can be applied [24], [25]. Indeed, since its introduction to the control community, this technique has distinguished itself by its high precision, simple implementation and little performance dependency on system parameters. Furthermore, thanks to a great effort to its theoretical development and to various algorithms that have been proposed in the last years, a lot of engineering problems (e.g., wind turbines control) are now treated with a repetitive control model [15]-[17].

In Fig. 2 the functional scheme of a repetitive controller approach is shown. The block $C_{rc}(s)$ is usually added to an existing feedback control system and is composed of a free time-delay system e^{-Ts} in a positive feed-back loop, and a low-pass filter $q(s)$. It should be noticed that, while the time-delay term is well known for decreasing the stability

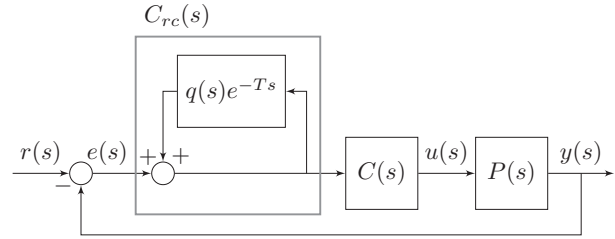


Fig. 2 Repetitive control scheme

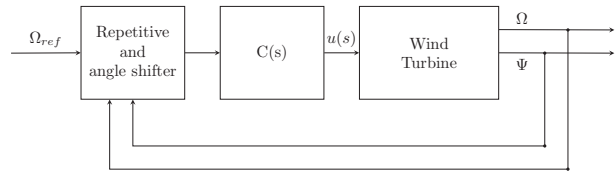


Fig. 3 Spatial repetitive control scheme

margin, on the other hand the low pass filter is added to ensure stability. In particular, the repetitive control loop in Fig. 2 is equivalent to the modified version proposed by Hara in [26], with $a(s) = 1$, which sacrifices tracking performances at high frequencies for system stability.

In this paper, a modified repetitive control strategy is applied on the model proposed in Section II.

D. The Proposed Repetitive Controller

The design of the controller follows the procedure detailed in [27]-[29] where a phase shifting is considered. To this aim, the free time delay system in Fig. 2 has been modified as

$$e^{-(T-\gamma_k)} \quad (8)$$

where T is the period of the signal and γ_k is a phase shifting of k samples of the same periodic signal.

It should be noticed that, the phase shifting technique is particularly useful in non-minimum phase systems, such as flexible structures. In fact, using the phase shifting, the iterative algorithm could reach the convergence also at high frequencies. Moreover, in [30] it has been shown that iterative learning algorithms are sub-optimal, converging with a small error, for quasi-linear systems with small non-linearity.

During the validation steps of the model presented in Section II (without the action of a feedback control loop), the authors observed a periodic trend of the pitch angle due to the effect of the gravitational force (see Section IV). Hence, they preferred to apply a *spatial* collective repetitive control algorithm to counterbalance this periodic trend. The term *spatial* refers to the azimuth angle on which the controller acts. In fact, recent studies [31]-[34], have shown that a spatial-based repetitive controller can be used, without degrading its performances, in combination with systems operating at varying speed. Notice that, in our case study, the shifting of k samples depends both on the rotor angular velocity Ω and on the rotor azimuth angle Ψ (see Fig. 3).

The collective repetitive controller has also been coupled with a $C(s) = PD(s)$, in order to dampen oscillations of the

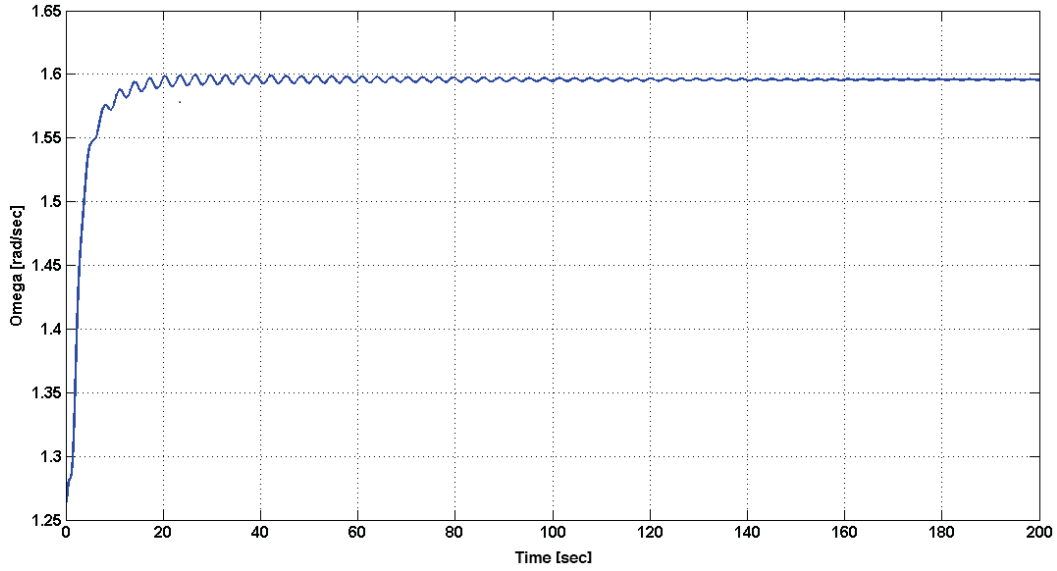


Fig. 4 Open-Loop convergence of angular velocity

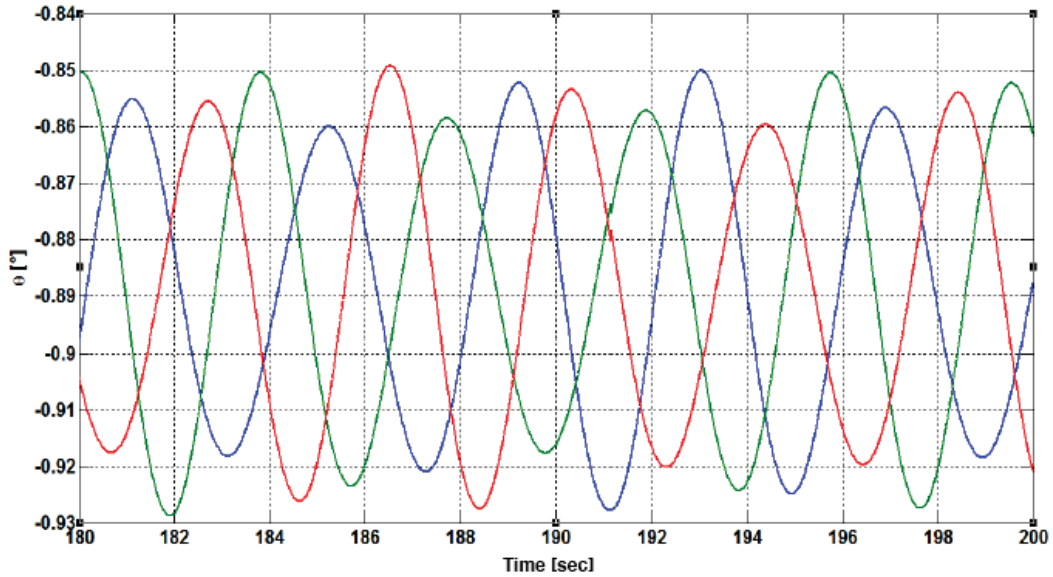


Fig. 5 Open-Loop steady solution of pitch angle for the three blades

blades and to satisfy the quasi-linearity constraint supposed by [30].

Algorithm 1 shows the proposed *spatial* repetitive control algorithm. Notice, at line 5, the shift of 35 samples.

IV. SIMULATIONS AND VALIDATION

In this section the validation of the proposed model (open-loop results) is presented along with the assessment of controller efficiency (closed loop simulations). In order to validate the model introduced in Section II the authors considered a 5 MW HAWT, characterized by radius $R = 61.5$ m and by mean chord $c = 3$ m. The first analysis performed is the steady state solution, considering a uniform wind $V_w = 11.4$ m/s and imposing collective pitch angle

Algorithm 1: Spatial Repetitive

Buffer : x, x_{new} (actual and new state)
Init : $x = [0, \dots, 0]$ (control signal buffer)
Input : $[e, \Psi]$ (actual error and azimuth angle)
Output : u (control signal)

```

1 if  $\Psi$  has changed of 0.5 degrees then
2   for  $i = 1 : (2 * 360 - 1)$  do
3      $x_{new}(i) = x(i + 1)$ ;
4   end
5   shift = 35;
6    $x_{new}(2 * 360 - 2 * \text{shift}) = x(2 * 360 + 1 - 2 * \text{shift}) + e$ ;
7    $x_{new}(2 * 360) = x(1)$ ;
8 else
9    $x_{new} = x$ ;
10 end
11  $u = x_{new}(1)$ ;

```

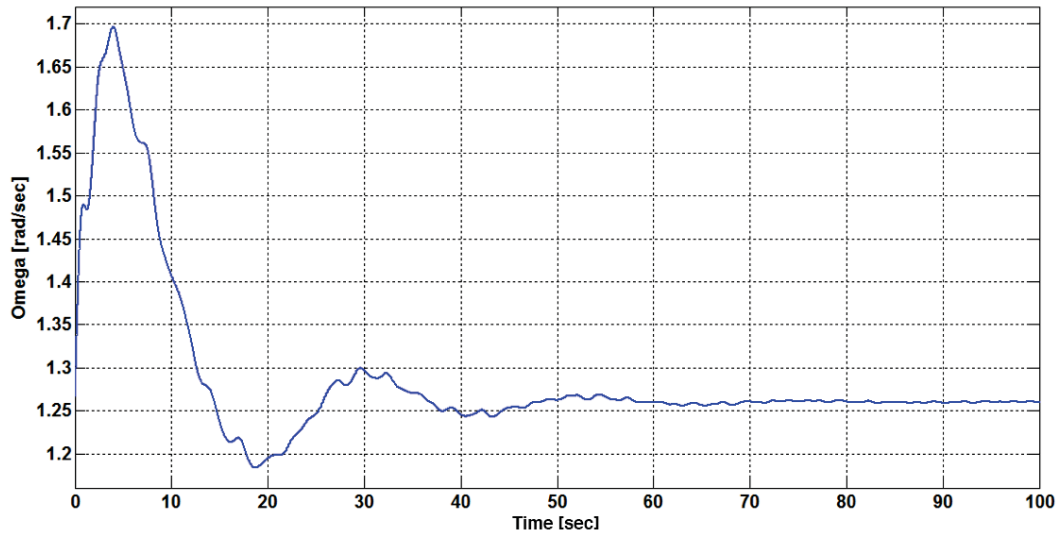


Fig. 6 Angular velocity when the PD-controller acts to reject Ω variation induced by an increase in wind speed

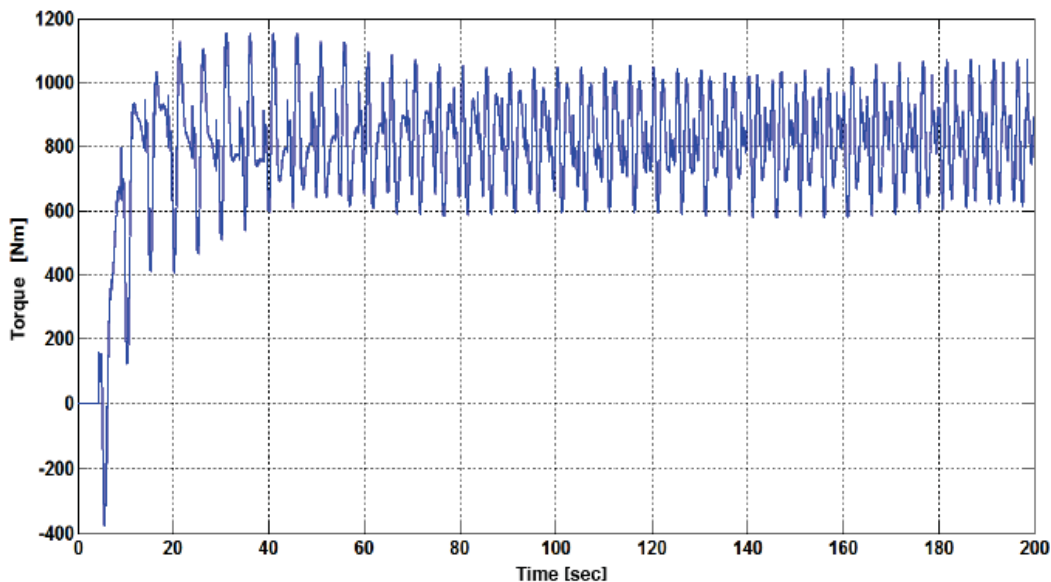


Fig. 7 Control torque applied to obtain Ω shown in Fig. 6

$\theta = -0.88^\circ$. Fig. 4 show the time-history of the angular velocity Ω and its equilibrium value (1.6 rad/s) over 200 s of simulation. This value is near to that reported in FAST documentation [35] for the same turbine.¹ Fig. 5 shows the almost-periodic solution of the pitch angle, when the blade rotation is constrained with a rotational spring about $\theta = -0.88^\circ$ (instead of being clamped). The periodicity of the system is clearly dominated by the Ω frequency and the phases between consecutive blades solutions are all equal to $1/3$ of the period of revolution.

Next, the effectiveness of the controller presented in Section III-C is assessed. The gains of the PD controller coupled with the repetitive one are reported in the first row of Table I.

¹FAST is a well-known, high fidelity aeroelastic code for HAWT analysis, considering a much higher number of dofs.

TABLE I
CONTROLLERS GAINS

Gains	P	I	D
Repetitive PD	-0.018	0	-0.01
Standard PID	-0.018	-0.00114	0

Starting from wind speed velocity $V_w = 11.4$ m/s the controller was asked to maintain the nominal angular velocity $\Omega_n = 1.266$ rad/s after an instantaneous increase of wind speed ($V_w = 15$ m/s). Fig. 6 shows the results in terms of the angular velocity. Note that, after a 20 s-long transient, the angular velocity returns to its nominal value.

Figs. 7 and 8 show the control torque and the resulting pitch angle under the action of the PD-repetitive controller. Then, a purely periodic external disturbance (having period

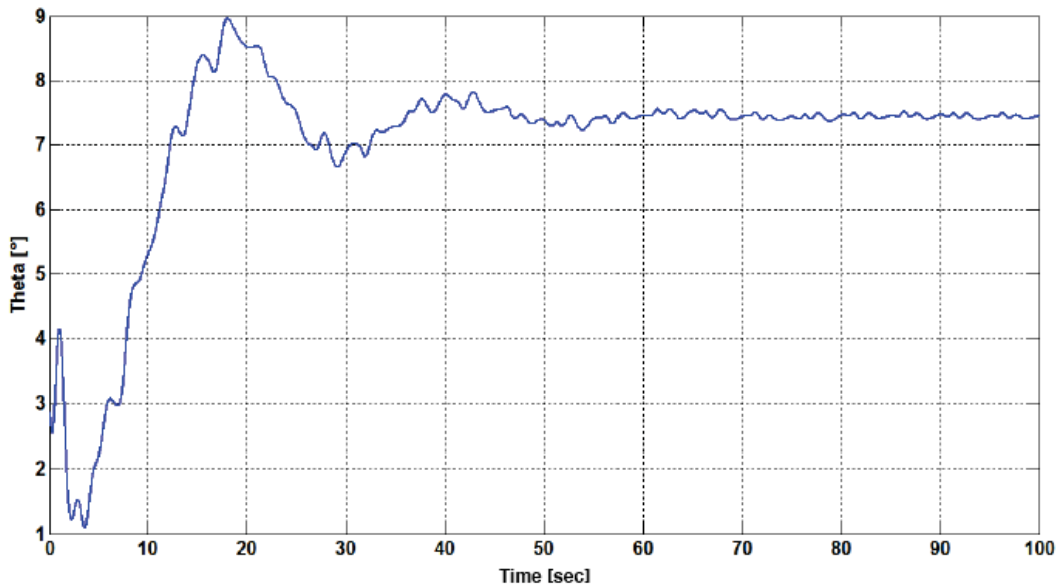


Fig. 8 Blade pitch resulting from the application of control torque shown in Fig. 7

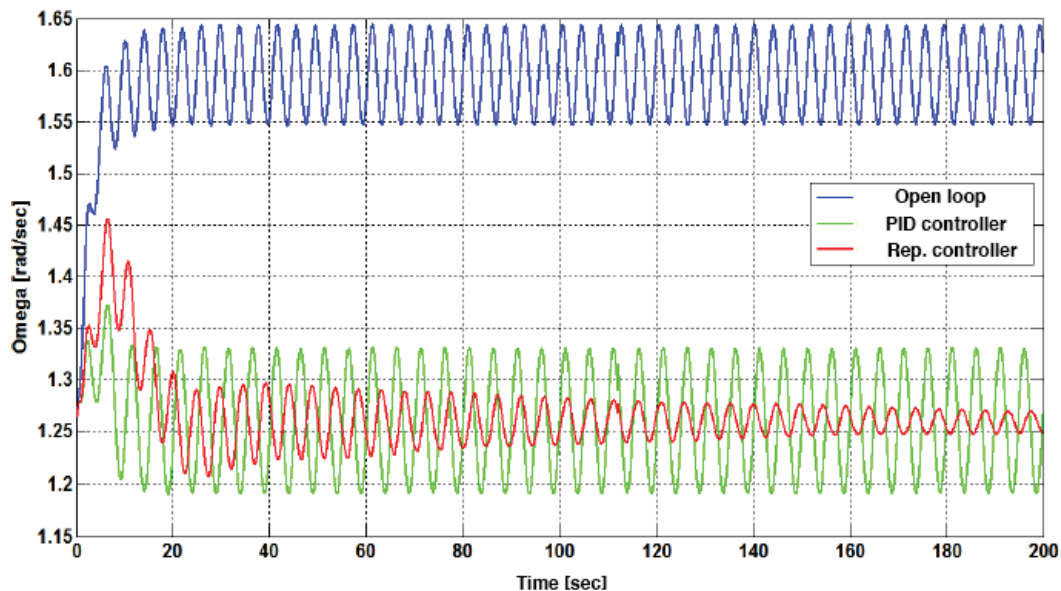


Fig. 9 Angular velocity in presence of periodic torque disturbance

$\Psi = 2\pi$) on generator torque is introduced in order to stress the capabilities of the repetitive controller. The performance of the *spatial* repetitive controller is compared with that of a PI controller alone (the gains of this controller are reported in the second row of Table I). Figs. 9 and 10 show the outcome of the closed loop simulation, in terms of angular velocity and power output, respectively. In particular, the behavior of Ω without the control is depicted in blue, while the two control approaches are identified by green line (PI) and red line (repetitive-PD). It is evident that, while the mean values of both controlled cases match the requirement, only the repetitive controller is able to reject the periodic disturbance.

V. CONCLUSIONS

In this paper, the authors presented a nonlinear differential aerolastic model for a three-bladed HAWT. The model is obtained through the Euler-Lagrange equation, whereas the expressions of the aerodynamic loads are obtained using quasi-steady strip theory. In the open loop simulations on a 5 MW HAWT, the model has given predictions in good agreement with those from high-fidelity commercial codes.

A *spatial* repetitive-PD controller acting on collective pitch algorithm is also proposed for the rejection of a periodic disturbance and of the periodicity characteristic of wind turbines. The results show that, contrary to a simple PI controller, the *spatial* repetitive-PD controller has the

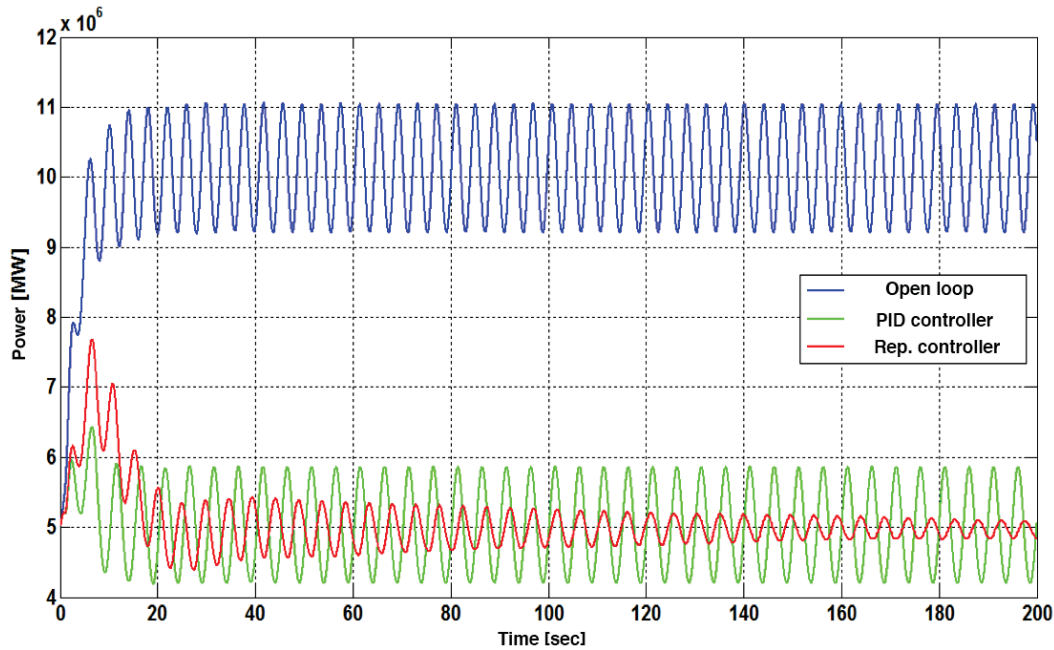


Fig. 10 Power output in presence of torque disturbance

capability to reject both kind of disturbances. Future work would include the improvement of aeroelastic model with: i) the inclusion of the variation of wind velocity due to terrain boundary layer; ii) the modeling of lag motion of the blades, which plays a crucial role in aeroelastic stability; iii) the capability to model rotors with unbalanced blades (*e.g.* due to mechanical or structural problems during life cycle). On the control side, a weighted repetitive collective blade pitch controller could be used, in order to remove the residual error on the pitch mode.

SYMBOLS

Below is a list of frequently used symbols and their definitions.

z_p	Translation of the pylon
β	Flapping angle
θ	Pitch angle
ψ	Azimuth angle
Ω	Angular velocity
m_{tot}	Sum of nacelle and pylon mass
m_b	Blade mass
J_{gb}	Blade matrix of inertia
k_p	Elastic constant of the pylon motion
k_β	Elastic constant of the flapping motion
k_θ	Elastic constant of the pitching motion
L	Aerodynamic force
M	Aerodynamic moment
C_c	Pitch control torque
f	Hinge offset
ϕ	Blade twist
c	Airfoil chord
ρ	Air density
V_w	Wind velocity
r	Coordinate along blade span

REFERENCES

- [1] F. D. Bianchi, H. De Battista, and R. J. Mantz, *Wind turbine control systems: principles, modelling and gain scheduling design*. Springer Science & Business Media, 2006.
- [2] J. Leishman, "Challenges in modeling the unsteady aerodynamics of wind turbines," 2002.
- [3] M. Carrin, R. Steijl, M. Woodgate, G. Barakos, X. Munduate, and S. Gomez-Iradi, "Aeroelastic analysis of wind turbines using a tightly coupled cfd-csd method," *Journal of Fluids and Structures*, vol. 50, pp. 392–415, 2014.
- [4] D. Yu and O. Kwon, "Predicting wind turbine blade loads and aeroelastic response using a coupled cfd-csd method," *Renewable Energy*, vol. 70, pp. 184–196, 2014.
- [5] M. Gennaretti and G. Bernardini, "Novel boundary integral formulation for blade-vortex interaction aerodynamics of helicopter rotors," *AIAA Journal*, vol. 45, no. 6, pp. 1169–1176, 2007.
- [6] L. Greco, R. Muscarelli, C. Testa, and A. Di Mascio, "Marine propellers performance and flow-field prediction by a free-wake panel method," *Journal of Hydrodynamics*, vol. 26, no. 5, pp. 780–795, 2014.
- [7] M. C. M. G. L. Calabretta, A. and M. Gennaretti, "Assessment of a comprehensive aeroelastic tool for horizontal-axis wind turbine rotor analysis," in press.
- [8] C. Bottasso, A. Croce, B. Savini, W. Sirchi, and L. Trainelli, "Aero-servo-elastic modeling and control of wind turbines using finite-element multibody procedures," *Multibody System Dynamics*, vol. 16, no. 3, pp. 291–308, 2006.
- [9] D. Schlipf, D. Schlipf, and M. Khn, "Nonlinear model predictive control of wind turbines using lidar," *Wind Energy*, vol. 16, no. 7, pp. 1107–1129, 2013.
- [10] J. Mullen and J. Hoagg, "Wind turbine torque control for unsteady wind speeds using approximate-angular-acceleration feedback," 2013.
- [11] E. Bossanyi, P. Fleming, and A. Wright, "Field test results with individual pitch control on the nrel cart3 wind turbine," 2012.
- [12] E. Bossanyi, "Individual blade pitch control for load reduction," *Wind Energy*, vol. 6, no. 2, pp. 119–128, 2003.
- [13] V. Rezaei and K. Johnson, "Robust fault tolerant pitch control of wind turbines," 2013.
- [14] S. Gros, "An economic nmpc formulation for wind turbine control," 2013.
- [15] J. Friis, E. Nielsen, J. Bonding, F. Adegas, J. Stoustrup, and P. Odgaard, "Repetitive model predictive approach to individual pitch control of wind turbines," in *Decision and Control and European Control Conference (CDC-ECC), 2011 50th IEEE Conference on*, Dec 2011.

- [16] H. Hosseini and M. Kalantar, "Repetitive control scheme for an ecs to improve power quality of grid connected wind farms using svm," in *Smart Grids (ICSG), 2012 2nd Iranian Conference on*, May 2012.
- [17] I. Houtzager, J. W. van Wingerden, and M. Verhaegen, "Rejection of periodic wind disturbances on a smart rotor test section using lifted repetitive control," *IEEE Transactions on Control Systems Technology*, vol. 21, no. 2, pp. 347–359, March 2013.
- [18] J. M. Greenberg, "Airfoil in sinusoidal motion in a pulsating stream," 1947.
- [19] T. Theodorsen, "General theory of aerodynamic instability and the mechanism of flutter," 1949.
- [20] D. Hodges and R. ORMISTON, "Stability of elastic bending and torsion of uniform cantilevered rotor blades in hover," in *14th Structures, Structural Dynamics, and Materials Conference*, 1973, p. 405.
- [21] D. A. Spera, "Wind turbine technology," 1994.
- [22] J. H. Laks, L. Y. Pao, and A. D. Wright, "Control of wind turbines: Past, present, and future," in *American Control Conference, 2009. ACC'09. IEEE*, 2009, pp. 2096–2103.
- [23] J. Ringwood and S. Simani, "Overview of modelling and control strategies for wind turbines and wave energy devices: Comparisons and contrasts," *Annual Reviews in Control*, vol. 40, pp. 27–49, 2015.
- [24] T. Y. Doh and J. Ryoo, "Robust repetitive controller design and its application on the track-following control system in optical disk drives," in *Decision and Control and European Control Conference (CDC-ECC), 2011 50th IEEE Conference on*, Dec 2011.
- [25] L. Cuiyan, Z. Dongchun, and Z. Xianyi, "Theory and applications of the repetitive control," in *SICE 2004 Annual Conference*, vol. 1, 2004.
- [26] S. Hara, Y. Yamamoto, T. Omata, and M. Nakano, "Repetitive control system: a new type servo system for periodic exogenous signals," *IEEE Transactions on Automatic Control*, vol. 33, no. 7, pp. 659–668, Jul 1988.
- [27] M. Poloni and G. Ulivi, "Iterative trajectory tracking for flexible arms with approximate models," in *Advanced Robotics, 1991. 'Robots in Unstructured Environments', 91 ICAR., Fifth International Conference on*, June 1991.
- [28] A. Carozzi, A. Fioretti, M. Poloni, F. Nicolo, and G. Ulivi, "Implementation of a tracking learning controller for an industrial manipulator," in *Control Applications, 1993., Second IEEE Conference on*, Sep 1993.
- [29] S. Panzieri and G. Ulivi, "Disturbance rejection of iterative learning control applied to trajectory tracking for a flexible manipulator," in *European Control Conf. (ECC 1995)*, Roma, Italy, September 1995.
- [30] P. Lucibello, S. Panzieri, and F. Pascucci, "Suboptimal output regulation of robotic manipulators by iterative learning," in *11th Int. Conf. on Advanced Robotics*, 2003, iLC.
- [31] Y.-H. Yang and C.-L. Chen, "Spatially periodic disturbance rejection using spatial-based output feedback adaptive backstepping repetitive control," 2008.
- [32] C.-L. Chen, G.-C. Chiu, and J. Allebach, "Robust spatial-sampling controller design for banding reduction in electrophotographic process," *Journal of Imaging Science and Technology*, vol. 50, no. 6, pp. 530–536, 2006.
- [33] B. Mahawan and Z.-H. Luo, "Repetitive control of tracking systems with time-varying periodic references," *International Journal of Control*, vol. 73, no. 1, pp. 1–10, 2000.
- [34] M. Nakano, J.-H. She, Y. Mastuo, and T. Hino, "Elimination of position-dependent disturbances in constant-speed-rotation control systems," *Control Engineering Practice*, vol. 4, no. 9, pp. 1241–1248, 1996.
- [35] J. M. Jonkman and M. L. Buhl Jr, "Fast users guide," *National Renewable Energy Laboratory, Golden, CO, Technical Report No. NREL/EL-500-38230*, 2005.